

**STOCHASTIC MODELLING OF BIOETHANOL
FERMENTATION BY *SACCHAROMYCES*
CEREVISIAE GROWN IN OIL PALM RESIDUES**

MOHD DINIE MUHAJIMIN BIN SAMSUDIN

UNIVERSITI SAINS MALAYSIA

2015

**STOCHASTIC MODELLING OF BIOETHANOL FERMENTATION BY
SACCHAROMYCES CEREVISIAE GROWN IN OIL PALM RESIDUES**

by

MOHD DINIE MUHAJMIN BIN SAMSUDIN

**Thesis submitted in fulfillment of the requirements for the degree of
Doctor of Philosophy**

MARCH 2015

ACKNOWLEDGEMENTS

Alhamdulillah, all praises to Allah S.W.T, the most gracious and the most merciful, and may peace blessings of Allah be upon His messenger, Prophet Muhammad S.A.W. First and foremost, I would like to express my gratitude to His greatness, with whose indulgence has given me the strength and convenience to complete this research successfully. The writing of this thesis has been one of the most significant academic challenges I have ever had to face. It has been seen through to completion with the support and encouragement from numerous people whom I am thankful for. First and foremost, I would like to express my sincere gratitude to my supervisor Professor Dr. Mashitah Mat Don for her continuous support of my PhD study and research, for her patience, motivation, enthusiasm and immense knowledge. Her guidance helped me in all the time of research and writing of this thesis. I would also like to thank her for being an open person to ideas, and for encouraging and helping me to shape my interest and ideas. The completion of this thesis would not have been possible without her unreserved help and supervision. One simply could not wish for a better and friendlier supervisor. I am indebted to her more than she knows.

I would like to pay homage to the Dean of School of Chemical Engineering, USM, Professor Dr. Azlina Harun @ Kamaruddin for her support and help concerning my postgraduate affairs. I am also very much thankful to all staff and technicians of School of Chemical Engineering for their co-operation and warmest helping hand for the past few years. Not to forget, I would also like to extend my gratitude to all staff of the Serting Hilir Palm Oil Mill especially the Assistant

Manager, Mr. Mohd Hafiz Bin Abd Kadir for providing palm oil mill effluent, and the staff of Forest Research Institute of Malaysia, for providing oil palm trunk sap. Words fail me to express my heart-felt gratitude to all my fellow friends and colleagues, who were always been great support in all my struggles and frustrations along my study. We could always share problems, excitement and supports among each other. Thank you so much for the friendship and memories.

Last but not least, my deepest gratitude goes to my beloved family, especially my parents (Samsudin Bin Ngah and Wan Rahami Binti Wan Abdullah) and siblings for their endless love and support that they have shown without fail for the entire duration of my postgraduate study. A deep of gratitude and love should be given to my dear and beloved wife, Umami Nadzirah Binti Hamzah, and our adorable daughter, Nur Zara Irdina Binti Mohd Dinie Muhaimin. I owe everything to them for providing me a carefree environment to concentrate on my study. Even though they could hardly understand what my research is all about, they are always there for me with sincere encouragement and inspiration throughout my research work and lifting me uphill this phase of life. Thank you so much to cheer me up and stand by me through all the good and bad times. Finally, I appreciate the financial support provided by Universiti Teknologi Malaysia and Ministry of Education, Malaysia throughout my postgraduate study. I would like to thank everybody who was important to the successful realization of this thesis. Your kindness shall not be forgotten. Thank you very much.

Mohd Dinie Muhaimin Bin Samsudin

March 2015

TABLE OF CONTENTS

	Page
ACKNOWLEDGEMENTS	ii
TABLE OF CONTENTS	iv
LIST OF TABLES	xi
LIST OF FIGURES	xiv
LIST OF PLATES	xxi
LIST OF ABBREVIATIONS	xxii
LIST OF SYMBOLS	xxv
ABSTRAK	xxviii
ABSTRACT	xxx
CHAPTER 1 – INTRODUCTION	
1.1 Research background	1
1.2 Problem statement	4
1.3 Research objectives	6
1.4 Scope of study	7
1.5 Organization of the thesis	9
CHAPTER 2 – LITERATURE REVIEW	
2.1 Bioethanol	12
2.1.1 Bioethanol fermentation	15
2.1.2 Sources of feedstock	22
2.1.2 (a) Lignocellulosic materials	22

2.1.2 (b) Algae	27
2.1.2 (c) Starch	29
2.1.2 (d) Wastes	31
2.1.3 Environmental variables affecting bioethanol fermentation	32
2.1.3 (a) Temperature	32
2.1.3 (b) Pressure	33
2.1.3 (c) pH	34
2.1.3 (d) Viscosity	36
2.1.3 (e) Nutrients	37
2.1.3 (f) Inoculum size	39
2.1.3 (g) Glucose concentration	40
2.1.3 (h) Ethanol concentration	40
2.2 Yeast as a model organism	41
2.2.1 <i>Saccharomyces cerevisiae</i>	41
2.2.2 Other fermenting microorganisms	42
2.2.3 Genetically engineered organisms	45
2.2.4 Response of yeast against stress	47
2.2.4 (a) Responses against osmotic stress	48
2.2.4 (b) Responses against ethanol toxicity	53
2.3 Oil palm residues	56
2.3.1 Oil palm trunk (OPT)	57
2.3.2 Palm oil mill effluent (POME)	58
2.3.3 Concentration of oil palm trunk (OPT) sap using rotary vacuum evaporator and evaporation kinetics models	61
2.4 Stochastic modelling and sensitivity analysis	64

2.4.1	Stochastic modelling using Monte Carlo algorithm	64
2.4.2	Sensitivity analysis	67
2.5	Summary	68
 CHAPTER 3 – MATERIALS AND METHODS		
3.1	Chemicals and equipment	70
3.2	Research methodology flowchart	72
3.3	Preparation of oil palm trunk (OPT) sap and palm oil mill effluent (POME)	74
3.4	Preparation of inoculum	75
3.5	Bioethanol fermentation	75
3.5.1	Shake-flask fermentation	75
3.5.1 (a)	Optimization using one-factor-at-a-time (OFAT) method	76
3.5.1 (b)	Optimization using a statistical tool, response surface methodology (RSM) via face centered central composite design (FCCCD)	77
3.5.2	Batch fermentation in a stirred-tank bioreactor	81
3.5.2 (a)	Functions and specification	81
3.5.2 (b)	Fermentation procedures	82
3.6	Stochastic modelling of bioethanol yield using Monte Carlo algorithm	83
3.6.1	Identification and definition of the mathematical model	84
3.6.2	Association of uncertainty of each variable	90
3.6.3	Creation or generation of random data	90
3.6.4	Simulation and analyses of process output	91

3.7	Sensitivity analysis	91
3.8	Evaporation of oil palm residues, and its kinetics modelling studies	92
3.8.1	Evaporation procedure	92
3.8.2	Evaporation kinetics models	93
3.8.2 (a)	First-order kinetic model	93
3.8.2 (b)	Exponential models	94
3.9	Bioethanol fermentation at very high gravity (VHG)	95
3.10	Analytical method	96
3.10.1	Determination of total soluble solid (TSS)	96
3.10.2	Measurement of biosolid concentration	96
3.10.3	Determination of glucose concentration	97
3.10.4	Determination of bioethanol	97
3.10.5	Determination of cell viability	98
3.10.6	Mineral content analysis	98
3.10.6 (a)	Total nitrogen	98
3.10.6 (b)	Phosphorus	98
3.10.6 (c)	Potassium	99
3.10.6 (d)	Magnesium, calcium, iron, boron, zinc, manganese, and copper	99
3.10.7	Enzyme assays	99
3.10.7 (a)	Trehalose-6-phosphate phosphatase (TPP) assay	99
3.10.7 (b)	Glycerol-3-phosphatase (G3Pase) assay	99
3.10.7 (c)	Phosphate assay	100
3.10.7 (d)	Protein assay	100

CHAPTER 4 – RESULTS AND DISCUSSIONS

4.1 Optimization of bioethanol production by <i>Saccharomyces cerevisiae</i> using oil palm trunk (OPT) sap supplemented with palm oil mill effluent (POME) as substrates	102
4.1.1 Proximate composition of oil palm trunk (OPT) sap and palm oil mill effluent (POME)	102
4.1.2 Bioethanol production by <i>Saccharomyces cerevisiae</i> in shake flasks culture	104
4.1.2 (a) Optimization using one-factor-at-a-time (OFAT) method	104
4.1.2 (a) (i) Effect of OPT sap to POME ratio	105
4.1.2 (a) (ii) Effect of inoculum size	107
4.1.2 (a) (iii) Effect of initial pH	109
4.1.2 (a) (iv) Effect of incubation time	110
4.1.2 (b) Optimization using a statistical tool, response surface methodology (RSM) via face centered central composite design (FCCCD)	112
4.1.2 (b) (i) Development of regression model equation and statistical analysis	112
4.1.2 (b) (ii) Effect of process variables on bioethanol yield	117
4.1.2 (b) (iii) Optimum range of process variables and validation of model	122
4.1.3 Bioethanol production by <i>Saccharomyces cerevisiae</i> in a 2.5 L stirred-tank bioreactor	123

4.3.1 (a)	Fermentation performance	124
4.3.1 (b)	Effect of temperature	130
4.3.1 (c)	Effect of pH	131
4.3.1 (d)	Effect of agitation speed	132
4.2	Stochastic modelling of bioethanol yield from fermentation of oil palm trunk (OPT) sap and palm oil mill effluent (POME) by <i>Saccharomyces cerevisiae</i>	133
4.2.1	Identification of the mathematical model	134
4.2.1 (a)	<i>Saccharomyces cerevisiae</i> growth	142
4.2.1 (b)	Bioethanol production	143
4.2.1 (c)	Glucose consumption	143
4.2.2	Predictability evaluation using Monte Carlo simulation	144
4.3	Sensitivity analysis	146
4.3.1	Sensitivity analysis of kinetic parameter on bioethanol yield	146
4.3.2	Effect of process variables on bioethanol productivity	148
4.3.2 (a)	Effect of temperature	149
4.3.2 (b)	Effects of pH	152
4.3.2 (c)	Effects of agitation speed	153
4.4	Very high gravity (VHG) fermentation of oil palm trunk (OPT) sap and palm oil mill effluent (POME) by <i>Saccharomyces cerevisiae</i>	154
4.4.1	Oil palm residues concentrates behaviour studies	155
4.4.1 (a)	Effect of temperature and pressure on evaporation process	156
4.4.1 (b)	Model fitting and validation	159
4.4.1 (c)	Developed evaporation model	166

4.4.1 (d) Validation of developed model	170
4.4.1 (e) Changes of glucose concentration during rotary vacuum evaporation process	171
4.4.2 Response of <i>Saccharomyces cerevisiae</i> during very high gravity (VHG) fermentation	174
4.4.2 (a) Glycerol-3-phosphatase (G3Pase) activity	177
4.4.2 (b) Trehalose-6-phosphate phosphatase (TPP) activity	178
4.4.2 (c) Cell viability	180
 CHAPTER 5 – CONCLUSIONS AND RECOMMENDATIONS	
5.1 Conclusions	182
5.2 Recommendation for future researches	184
	186
 REFERENCES	
APPENDICES	216
Appendix A – Calibration curves	
Appendix B – Statistical analysis and graph plots	
Appendix C – Sample of calculations	
Appendix D – Software interface	
 LIST OF PUBLICATIONS	

LIST OF TABLES

	Page
Table 2.1 A review on bioethanol production conditions and bioethanol yield from fermentation by several microorganisms and substrates	16
Table 2.2 Algal sources for bioethanol production	28
Table 2.3 Un-dissociation of acids as affected by pH (Deak and Beuchat, 1996)	35
Table 2.4 POME discharge standards as required by the Environmental Quality Regulations (1974)	60
Table 3.1 List of chemicals	70
Table 3.2 List of equipment	72
Table 3.3 The experimental design for optimization using OFAT method	76
Table 3.4 List of range and levels of the experimental independent variables	77
Table 3.5 Experimental design matrix	79
Table 3.6 Desired goal of each factors and responses	80
Table 3.7 Initial estimates procedures for parameters tested	90
Table 3.8 Adjusted parameter values for sensitivity analysis	91
Table 4.1 Proximate composition of OPT sap	103
Table 4.2 Proximate composition of POME	104
Table 4.3 Experimental design matrix	113
Table 4.4 Sequential model sum of squares	114
Table 4.5 Lack-of-fit test	115

Table 4.6	Statistic summary for all models	116
Table 4.7	Analysis of variances (ANOVA) for the quadratic model	116
Table 4.8	Optimum conditions	122
Table 4.9	Comparison between the experimental results with predicted data	123
Table 4.10	Kinetic parameters of bioethanol fermentation by <i>S. cerevisiae</i> from oil palm residues at different temperatures	136
Table 4.11	Kinetic parameters of bioethanol fermentation by <i>S. cerevisiae</i> from oil palm residues at different pH	137
Table 4.12	Kinetic parameters of bioethanol fermentation by <i>S. cerevisiae</i> from oil palm residues at different impeller tip speed	137
Table 4.13	Statistical error parameters	138
Table 4.14	Empirical constant for product formation (Shuler and Kargi, 2002)	143
Table 4.15	Predicted standard deviation of kinetic model parameters	145
Table 4.16	Effect of fluctuation of kinetic model parameter on distribution of bioethanol yield	146
Table 4.17	Impact of kinetic parameters toward bioethanol yield	147
Table 4.18	Effects of process variables on value of $\mu_m(X_m-X_o)$	149
Table 4.19	Initial estimates of evaporation rates and coefficients of the mathematical models	160
Table 4.20	Statistical errors for prediction of OPT sap concentration during rotary vacuum evaporation	161
Table 4.21	Equation constants value and statistical error parameters for the developed models	169

Table 4.22	Coefficients of the developed model	171
Table 4.23	Statistical errors of the developed model	171
Table 4.24	Coefficient for correlation and statistical errors in relationship of total soluble solid and glucose concentration during rotary vacuum evaporation	173
Table 4.25	Bioethanol production and yield from VHG fermentation	177

LIST OF FIGURES

	Page
Figure 2.1 Metabolic pathway of bioethanol fermentation through EMP pathway (Bai et al., 2008). Abbreviations: HK: hexokinase, PGI: phosphoglucoisomerase, PFK: phosphofructokinase, FBPA: fructose biphosphate aldolase, TPI: triose phosphate isomerase, GAPDH: glyceraldehydes-3-phosphate dehydrogenase, PGK: phosphoglycerate kinase, PGM: phosphoglyceromutase, ENO: enolase, PYK: pyruvate kinase, PDC: pyruvate decarboxylase, ADH: alcohol dehydrogenase.	20
Figure 2.2 Conversion of glucose into pyruvate	21
Figure 2.3 Conversion of pyruvate into bioethanol and carbon dioxide	21
Figure 2.4 Production of bioethanol from lignocellulosic materials (Galbe and Zacchi, 2002)	24
Figure 2.5 Starches	31
Figure 2.6 Routes of bioethanol fermentation from sugar: a) Embden–Meyerh-of–Parnas pathway; b) Entner-Doudoroff pathway; c) Heterofermentative pathway	45
Figure 2.7 Potential environmental stresses on yeast cell during bioethanol fermentation (Bai et al., 2008)	47
Figure 2.8 Schematic overview of fermentative and oxidative glucose metabolism of <i>Saccharomyces cerevisiae</i>	51

Figure 2.9	The pathway for glycerol synthesis from dihydroxyacetone phosphate, and glycerol dissimilation. Abbreviation: ADP, Adenosine diphosphate; G3PDH-M, mitochondrial glycerol-3-phosphate dehydrogenase; GK, glycerol kinase; GDH, glycerol dehydrogenase; DK, dihydroxyacetone kinase	52
Figure 2.10	Enzymatic reactions involved in the biosynthesis and the dissimilation of trehalose	55
Figure 3.1	Process flow diagram of research methodology	73
Figure 3.2	Piping and instrumentation diagram of bioreactor	82
Figure 3.3	Rushton turbine impeller	82
Figure 3.4	Process flow diagram of stochastic modelling study	83
Figure 4.1	Effect of OPT sap to POME ratio on bioethanol yield by <i>S. cerevisiae</i>	105
Figure 4.2	Effect of inoculum size on bioethanol yield by <i>S. cerevisiae</i> in a mixture of OPT sap and POME	108
Figure 4.3	Effect of initial pH on bioethanol yield by <i>S. cerevisiae</i> in a mixture OPT sap and POME	109
Figure 4.4	Effect of incubation time on growth, glucose consumption, and bioethanol yield by <i>S. cerevisiae</i> grown on OPT sap and POME (● Glucose concentration; ■ Bioethanol yield; ▲ Biosolid concentration)	111
Figure 4.5	Perturbation plot of bioethanol yield	118
Figure 4.6	Response surface and contour plot of bioethanol yield as a function of OPT sap to POME ratio and incubation time at initial medium pH 8.0 and inoculum size 4% (v/v)	120

Figure 4.7	Response surface and contour plot of bioethanol yield as a function of inoculum size and initial medium pH at inoculum size 4% (v/v) and incubation time 120 hours	120
Figure 4.8	Response surface and contour plot of bioethanol yield as a function of inoculum size and incubation time at initial medium pH 8.0 and inoculum size 4% (v/v)	121
Figure 4.9	Response surface and contour plot of bioethanol yield as a function of initial pH and incubation time at OPT sap to POME ratio of 60:40 and inoculum size 4% (v/v)	121
Figure 4.10	Effect of different temperature on (a) biosolid concentration, (b) bioethanol production, and (c) glucose consumption by <i>S. cerevisiae</i> in a 2.5 L stirred tank bioreactor. ♦ 27°C; ■ 30°C; ▲ 33°C; X 36°C; and ● 39°C (Condition: pH 7.0, agitation speed 0.3 m/s impeller tip speed)	125
Figure 4.11	Effect of different pH on (a) biosolid concentration, (b) bioethanol production, and (c) glucose consumption by <i>S. cerevisiae</i> in a 2.5 L stirred tank bioreactor. ♦ pH 6.0; ■ pH 6.5; ▲ pH 7.0; X 7.5; and ● pH 8.0 (Condition: temperature 33°C, agitation speed 0.3 m/s impeller tip speed)	126
Figure 4.12	Effect of different agitation speed on (a) biosolid concentration, (b) bioethanol production, and (c) glucose consumption by <i>S. cerevisiae</i> in a 2.5 L stirred tank bioreactor. ♦ 0.1; ■ 0.2; ▲ 0.3; X 0.4; and ● 0.5 m/s impeller tip speed (Condition: temperature 33°C, pH 7.0)	127

Figure 4.13	Typical yeast cell growth curve during fermentation (Bamforth and Ward, 2014)	128
Figure 4.14	Simulated and experimental data for (a) biosolid concentration, (b) bioethanol production, and (c) glucose consumption during fermentation by <i>S. cerevisiae</i> at different temperatures. ♦ , — 27°C; ■ , 30°C; ▲ , ---- 33°C; X , --- 36°C; and ● , -.- 39°C (dots – experimental data, lines – simulated curve)	139
Figure 4.15	Simulated and experimental data for (a) biosolid concentration, (b) bioethanol production, and (c) glucose consumption during fermentation by <i>S. cerevisiae</i> at different pH. ♦ , — pH 6.0; ■ , pH 6.5; ▲ , ---- pH 7.0; X , --- pH 7.5; and ● , -.- pH 8.0 (dots – experimental data, lines – simulated curve)	140
Figure 4.16	Simulated and experimental data for (a) biosolid concentration, (b) bioethanol production, and (c) glucose consumption during fermentation by <i>S. cerevisiae</i> at different agitation speeds. ♦ , — 0.1 m/s; ■ , 0.2 m/s; ▲ , ---- 0.3 m/s; X , --- 0.4 m/s; and ● , -.- 0.5 m/s impeller tip speed (dots – experimental data, lines – simulated curve)	141
Figure 4.17	Plot of $\ln(\mu_m(X_m - X_o))$ against $1/T$	151
Figure 4.18	Relationship between $\mu_m(X_m - X_o)$ and pH/pH_{opt}	153
Figure 4.19	Relationship between $\mu_m(X_m - X_o)$ and agitation speed	154

Figure 4.20	Effect of evaporation temperature on the oil palm trunk sap concentration in a rotary vacuum evaporator at 120 mbar.absolute (◆ 70°C, ■ 65°C, ▲ 60°C, ● 55°C, X 50°C)	156
Figure 4.21	Effect of evaporation pressure on the OPT sap concentration in a rotary vacuum evaporator at 60°C (◆ 70 mbar.absolute, ■ 95 mbar.absolute, ▲ 120 mbar.absolute, ● 145 mbar.absolute, X 170 mbar.absolute)	157
Figure 4.22	Concentration profiles of OPT sap in rotary vacuum evaporator at different temperature using first-order kinetic model at 120 mbar.absolute (◆ 70°C, ■ 65°C, ▲ 60°C, ● 55°C, X 50°C)	162
Figure 4.23	Concentration profiles of OPT sap in rotary vacuum evaporator at different temperature using two-parameter exponential model at 120 mbar.absolute (◆ 70°C, ■ 65°C, ▲ 60°C, ● 55°C, X 50°C)	162
Figure 4.24	Concentration profiles of OPT sap in rotary vacuum evaporator at different temperature using three-parameter exponential model at 120 mbar.absolute (◆ 70°C, ■ 65°C, ▲ 60°C, ● 55°C, X 50°C)	163
Figure 4.25	Concentration profiles of OPT sap in rotary vacuum evaporator at different temperature using four-parameter exponential model at 120 mbar.absolute (◆ 70°C, ■ 65°C, ▲ 60°C, ● 55°C, X 50°C)	163

Figure 4.26	Concentration profiles of OPT sap in rotary vacuum evaporator at different pressure using first-order kinetic model at 60°C (♦ 70 mbar.absolute, ■ 95 mbar.absolute, ▲ 120 mbar.absolute, ● 145 mbar.absolute, X 170 mbar.absolute)	164
Figure 4.27	Concentration profiles of OPT sap in rotary vacuum evaporator at different pressure using two-parameter exponential model at 60°C (♦ 70 mbar.absolute, ■ 95 mbar.absolute, ▲ 120 mbar.absolute, ● 145 mbar.absolute, X 170 mbar.absolute)	164
Figure 4.28	Concentration profiles of OPT sap in rotary vacuum evaporator at different pressure using three-parameter exponential model at 60°C (♦ 70 mbar.absolute, ■ 95 mbar.absolute, ▲ 120 mbar.absolute, ● 145 mbar.absolute, X 170 mbar.absolute)	165
Figure 4.29	Concentration profiles of OPT sap in rotary vacuum evaporator at different pressure using four-parameter exponential model at 60°C (♦ 70 mbar.absolute, ■ 95 mbar.absolute, ▲ 120 mbar.absolute, ● 145 mbar.absolute, X 170 mbar.absolute)	165
Figure 4.30	Relationship between heating temperature (▲), and saturated vapour temperature (●) on the evaporation rate	167
Figure 4.31	Correlation between total soluble solid (TSS) and glucose concentration in OPT sap concentrate	172

Figure 4.32	Effect of different glucose concentration on the biosolid concentration. ♦ 100 g/L; ■ 150 g/L; ▲ 200 g/L; X 250 g/L; and ● 300 g/L	175
Figure 4.33	Effect of different glucose concentration on the bioethanol production. ♦ 100 g/L; ■ 150 g/L; ▲ 200 g/L; X 250 g/L; and ● 300 g/L	175
Figure 4.34	Effect of different glucose on the glucose consumption. ♦ 100 g/L; ■ 150 g/L; ▲ 200 g/L; X 250 g/L; and ● 300 g/L	176
Figure 4.35	Effect of different glucose concentration on the activity of glycerol-3-phosphatase (G3Pase) enzyme. ♦ 100 g/L; ■ 150 g/L; ▲ 200 g/L; X 250 g/L; and ● 300 g/L	178
Figure 4.36	Effect of different glucose concentration on the activity of trehalose-6-phosphate phosphatase (TPP) enzyme ♦ 100 g/L; ■ 150 g/L; ▲ 200 g/L; X 250 g/L; and ● 300 g/L	180
Figure 4.37	Effect of different glucose concentration on the cell viability ♦ 100 g/L; ■ 150 g/L; ▲ 200 g/L; X 250 g/L; and ● 300 g/L	181

LIST OF PLATES

	Page
Plate 3.1 Wood chipper	74
Plate 3.2 Hydraulic squeezer	75

LIST OF ABBREVIATIONS

Symbol	Description
ADH	Alcohol dehydrogenase
ANOVA	Analysis of variances
ATP	Adenosine triphosphate
BBD	Box-Behnken design
BOD	Biological oxygen demand
CCD	Central composite design
CO ₂	Carbon dioxide
COD	Chemical oxygen demand
CPO	Crude palm oil
DHAP	Dihydroxyacetone
DIC	Dissolved inorganic carbon
DK	Dihydroxyacetone kinase
EFB	Empty fruit bunch
EMP	Embden–Meyerh-of–Parnas
ENO	Enolase
FAD	Flavin adenine dinucleotide
FBPA	Fructose bisphosphate aldolase
FCCCD	Face centered central composite design

FFB	Fresh fruit bunch
G3P	Form glycerol-3-phosphate
G3Pase	Glycerol-3-phosphatase
G3PDH	Glycerol-3-phosphate dehydrogenase
G3PDH-C	Cytoplasmic glycerol 3-phosphate dehydrogenase
G3PDH-M	Mitochondrial glycerol-3-phosphate dehydrogenase
GAP	Glyceraldehydes-3-phosphate
GAPDH	Glyceraldehydes-3-phosphate dehydrogenase
GDH	Glycerol dehydrogenase
GHG	Greenhouse gas
GK	Glycerol kinase
GRAS	Generally regarded as safe
HK	Hexokinase
HOG	High osmolarity glycerol
MAPK	Mitogen-activated protein kinase
NAD ⁺	Nicotinamide adenine dinucleotide
NADH	Nicotinamide adenine dinucleotide hydrate
OFAT	One-factor-at-a-time
OPEC	Organization of the Petroleum Exporting Countries
OPT	Oil palm trunk
PDC	Pyruvate decarboxylase

PFK	Phosphofructokinase
PGI	Phosphoglucoisomerase
PGK	Phosphoglycerate kinase
PGM	Phosphoglyceromutase
POME	Palm oil mill effluent
PYK	Pyruvate kinase
RMSE	Root-mean-square error
RSM	Response surface methodology
SHF	Separate hydrolysis and fermentation
SSF	Simultaneous saccharification and fermentation
T6P	Trehalose-6-phosphate
TPI	Triose phosphate isomerase
TPP	Trehalose-6-phosphate phosphatase
TPS	Trehalose-6-phosphate synthase
TSS	Total soluble solid
UDP-glucose	Uridine diphosphate glucose
VHG	Very high gravity

LIST OF SYMBOLS

Symbol	Description	Unit
ΔT	Temperature difference between the liquid and heater	Kelvin or °C
α (<i>Evaporation model</i>)	Constant	
α (<i>Kinetic model</i>)	Growth-associated product formation	g/g
β (<i>Evaporation model</i>)	Constant	
β (<i>Kinetic model</i>)	Non-growth-associated product formation	g/g.h
γ	Growth-associated substrate consumption coefficient	g/g
γ_i	Activity coefficient	-
δ	Non-growth-associated substrate consumption coefficient	g/g.h
ε	Statistical error	-
μ	Specific growth rate	hr ⁻¹
μ_m	Maximum specific growth rate	hr ⁻¹
A	Constant	-
B (<i>Antoine Equation</i>)	Constant	-
B (<i>Evaporation model</i>)	TSS concentration	°Brix
B_1	Constant	°Brix
B_o	Initial TSS concentration	°Brix
C (<i>Evaporation model</i>)	Constant	-
C (<i>Arrhenius Equation</i>)	Glucose concentration	g/L

D	Individual desirability	-
D	Total desirability	-
DF	Degrees of freedom	-
E_a	Activation energy	cal/mol
E_d	Thermal death activation energy	cal/mol
H	Effective heat transfer coefficient	W/m ² .K
k'	Rate constant	g/L.h
k (<i>Arrhenius Equation</i>)	pro-exponential factor of the fermentation rate constant	g/L.h
k (<i>Evaporation model</i>)	Evaporation rate	min ⁻¹
k_d	Kinetics thermal death	g/L.h
K_i	Equilibrium constant	-
M	Fermentation order	-
M	Moisture content	-
M_e	Equilibrium moisture content	-
M_o	Initial moisture content	-
MR	Moisture ratio	-
N	Agitation speed	rpm
N	Constant	
P	Product/bioethanol concentration	g/L
pH_{opt}	Optimum pH	-
P_{sat}	Saturated vapor pressure	mmHg
$P_{sat,i}$	Vapor pressure of component (i)	mmHg
Q	Heat transfer	W
R	Universal gas constant	cal/mol.K

S (<i>Kinetic model</i>)	Substrate/glucose concentration	g/L
S (<i>Predictability study</i>)	Response	-
S_o	Initial substrate/glucose concentration	g/L
SS	Sum of square	-
T	Temperature	Kelvin or °C
t (<i>Evaporation study</i>)	Time	minute
t (<i>Kinetic model</i>)	Time	hr
t_e	Time when exponential phase begins	hr
T_{max}	Maximum temperature	Kelvin or °C
T_{opt}	Optimal temperature	Kelvin or °C
T_{sat}	Saturated vapor temperature	Kelvin or °C
V_1	Bioethanol yield with all model parameters remained unchanged	g/g
V_2	Bioethanol yield with a single kinetic model parameter was adjusted	g/g
X	Biosolid concentration	g/L
x_i	Liquid molar fraction of component (i)	-
X_m	Maximum attainable biosolid concentration	g/L
X_o	Initial biosolid concentration	g/L
y_i	Vapor molar fraction of component (i)	-
$Y_{P/S}$	Yield coefficient of substrate for product formation	g/g
$Y_{X/S}$	Yield coefficient of substrate consumed for cell growth	g/g

**PEMODELAN STOKASTIK FERMENTASI BIOETANOL OLEH
SACCHAROMYCES CEREVISIAE DI DALAM SISA KELAPA SAWIT**

ABSTRAK

Dalam industri minyak sawit, batang kelapa sawit (OPT) dan efluen kilang kelapa sawit (POME) dihasilkan dalam kuantiti yang besar. Sisa-sisa ini tidak digunakan sepenuhnya, malah, dianggap sebagai bahan buangan yang akan membawa kepada pencemaran alam sekitar yang serius. Dalam kajian ini, didapati, perahan OPT mengandungi kandungan glukosa yang tinggi (49.08 – 49.16 g/L), dan POME mengandungi semua nutrien asas yang diperlukan oleh mikroorganisma. Maka, perahan OPT telah digunakan sebagai sumber karbon, manakala POME digunakan sebagai pembekal nutrien kepada proses fermentasi bagi menghasilkan bioetanol oleh *Saccharomyces cerevisiae*. Proses pengoptimuman di dalam kultur kelalang goncang menggunakan kaedah satu faktor pada satu masa (OFAT) menghasilkan hasil bioetanol sebanyak 0.428 g/g. Pengoptimuman kaedah permukaan tindak balas (RSM) melalui reka bentuk komposit berpusat - berpusatkan muka (FCCCD) juga telah dijalankan. Hasil bioetanol tertinggi (0.453 g/g) telah dicapai pada nisbah perahan OPT kepada POME 63:37, saiz inokulum 4.3% (v/v), pH permulaan 8.0, dan masa inkubasi selama 118 jam. Pengoptimuman kemudiannya telah dijalankan di dalam bioreaktor tangki teraduk berisipadu 2.5 L. Hasil tertinggi bioetanol (0.481 g/g) telah didapati pada 33°C, pH 7.0, and diaduk pada kelajuan hujung pendesak 0.4 m/s. Bagaimanapun, hasil ini mungkin berubah sekiranya ianya diulang disebabkan keheterogenan perahan OPT dan POME, dan juga kepelbagaian prestasi ibu roti. Maka, satu ujian kebolehjangkaan telah

dijalankan menggunakan algoritma Monte Carlo. Keputusan menunjukkan hasil bioetanol yang konsisten dengan kajian ini dapat dijangka sekiranya perubahan dalam parameter model kinetik adalah 2.5% atau kurang. Keberubahan melebihi 2.5% boleh menghasilkan variasi hasil bioetanol yang tinggi dengan sisihan piawai relatif melebihi 5.0%. Maka, analisis sensitiviti seterusnya telah dijalankan bagi menilai pengaruh setiap parameter model kinetik ke atas hasil bioetanol. Hasil menunjukkan hasil bioetanol amat bergantung kepada perubahan biopepejal yang mewakili perkembangan yis. Maka, bagi memaksimumkan hasil bioetanol, perkembangan yis mestilah diawasi dengan teliti. Bagi meningkatkan produktiviti bioetanol, fermentasi graviti amat tinggi (VHG) seterusnya telah dijalankan menggunakan perahan OPT dan POME yang dipekatkan. Dalam kajian ini, perahan OPT telah dipekatkan menggunakan penyejat vakum berputar. Sebagai tambahan, model penyejatan yang mengambil kira kedua-dua suhu dan tekanan telah dibangunkan dan disahkan. Didapati model yang dibangunkan bersesuaian bagi menerangkan perilaku penyejatan perahan OPT. Semasa fermentasi VHG, sehingga 131.2 mmol/(min.mg protein) aktiviti enzim glycerol-3-phosphatase (G3Pase) dan 60.5 mmol/(min.mg protein) aktiviti enzim trehalose-6-phosphate phosphatase (TPP) telah dikesan. Enzim-enzim ini dihasilkan oleh yis masing-masing untuk bertahan dalam tekanan osmosis tinggi, dan ketoksikan etanol tinggi.

STOCHASTIC MODELLING OF BIOETHANOL FERMENTATION BY *SACCHAROMYCES CEREVISIAE* GROWN IN OIL PALM RESIDUES

ABSTRACT

In oil palm industry, large quantity of oil palm trunk (OPT) and palm oil mill effluent (POME) are generated. These residues are not fully utilised, in fact, they serve as wastes leading to serious environmental pollution. In this study, it was found that OPT sap contained high glucose concentration (49.08 – 49.16 g/L), and POME contained all essential nutrients required by microorganisms. Therefore, OPT sap was used as carbon source, while POME was utilized as nutrient supplier for fermentation process to produce bioethanol by *Saccharomyces cerevisiae*. Process optimization in shake flasks culture using one-factor-at-a-time (OFAT) method produced bioethanol yield of 0.428 g/g. Response surface methodology (RSM) via face centered central composite design (FCCCD) optimization was also conducted. The highest bioethanol yield was achieved (0.453 g/g) at OPT sap to POME ratio of 63:37, inoculum size 4.3% (v/v), initial pH 8.0, and incubation time 118 hours. Optimization was then carried out in a 2.5 L stirred tank bioreactor. The highest bioethanol yield (0.481 g/g) was attained at 33°C, pH 7.0, and agitated at 0.4 m/s impeller tip speed. However, this result might differ if it is to be reduplicated due to heterogeneity of OPT sap and POME as well as variability in Baker's yeast's performance. Therefore, a predictability test was carried out using Monte Carlo algorithm. Results showed that consistence bioethanol yield with this study could be expected if the fluctuation of kinetic model parameters is 2.5% or below. Variability beyond 2.5% could result in high variation of bioethanol yield with relative standard

deviation of higher than 5.0%. Therefore, sensitivity analysis was then carried out in order to evaluate the influence of each kinetic model parameter on bioethanol yield. It showed that bioethanol yield highly dependent on the changes of biosolid which represented the yeast growth. Therefore, in order to maximise bioethanol yield, the yeast growth must be carefully monitored. In order to improve bioethanol production, very high gravity (VHG) fermentation was then carried out using concentrated OPT sap and POME. In this study, OPT sap was concentrated using a rotary vacuum evaporator. In addition, evaporation model considering both temperature and pressure was developed and validated. During VHG fermentation, up to 131.2 mmol/(min.mg protein) and 60.5 mmol/(min.mg protein) of glycerol-3-phosphatase (G3Pase) and trehalose-6-phosphate phosphatase (TPP) enzyme activity were detected, respectively. These enzymes were produced by Baker's yeast in order to sustain its growth in high osmotic stress, and high ethanol toxicity, respectively.

CHAPTER 1

INTRODUCTION

1.1 Research background

The demand for energy in Malaysia is increasing due to the incline of economic growth. As compared to the other developed countries, Malaysian's demand for energy is relatively high (Ong et al., 2011). The energy demand increased from 1243.7 Petajoule (PJ) in 2000 to 2217.9 PJ in 2010. To cope with the increment, energy supply has also been increased from 2003.1 PJ to 3127.7 PJ for the year 2000 to 2010 (Chua and Oh, 2010). Maximum energy demand was 10775 MW and 20870 MW for the year 2000 and 2010, respectively, and projected to 40515 MW in 2020 (Yusoff, 2006).

With the rapid growth of industrialization and urbanization, an efficient supply of energy at economically acceptable cost and sufficient quantity would be a vital concern in the energy sector (Sulaiman and Zain, 1996). Currently, Malaysia highly dependent on petroleum and coal as the source of energy since 1980s when petroleum and natural gas became the major contributor to Malaysia's economy following the collapse of tin market. As reported by Chua and Oh (2010), 47% of Malaysia's energy source is from petroleum based products, 41% from natural gas, 9% from coal and coke, and the rest are from hydropower.

Malaysia is ranked 24th in terms of world oil reserves and the 13th for natural gas reserves (Chua and Oh, 2010). Much of the oil reserves are situated off coast of

the Peninsular Malaysia, while much of the natural gas reserves come from East Malaysia, especially the offshore of Sarawak (Sulaiman et al., 2011). According to Mushtaq et al. (2013), Malaysia's oil reserves is only sufficient for the next 15.4 years, and natural gas reserves is only sufficient for the next 19.9 years. Consequently, the country's energy supply will be highly affected. Besides depleting oil and gas reserves, Malaysia energy sector also needs to face the increasing of oil price. In recent years, world price of crude oil and oil products in general have increased tremendously (Esmaeili and Shokoohi, 2011). As reported by FRED (2013), in January 1946 the oil price was 1.17 dollars per barrel as measured by continuous contract on the West Texas Intermediate and increased drastically to 104.61 dollars per barrel in July 2013.

Meanwhile, the country's coal resource is estimated to be around 1724 Mt (Million tonnes). Most of the reserves (80%) are located in East Malaysia and smaller amount are found in Selangor, Perlis and Perak of the Peninsular Malaysia. According to Sulaiman et al. (2011), the Malaysia's coal consumption is far higher than its production. Hence, Malaysia is importing coal mostly from Indonesia, Australia and China in order to meet the gap.

At the present time, sustainability becomes a crucial challenge facing by the energy sector (Singh et al., 2010). The sustainability of the sector is highly important to ensure the steady and reliability of energy supply and the diversification of energy sources (Ong et al., 2011). A lot of efforts must be made towards sustainable development in energy sector including efficient energy usage and reduction of energy wastage (Klemeš et al., 2010). However, a reduction in energy intensity alone

would not contribute much in sustainability. Renewable energy is believed to be the key to achieve energy sustainability (Kamarudin et al., 2009). Furthermore, some expert thought that solar, wind, and small-scale hydropower are not economically viable. For instance, solar electric prices in the USA today are approximately \$0.30/kWh which is about 2–5 times the average residential electricity tariffs due to the high installation costs (Devabhaktuni et al., 2013). Moreover, Singh and Erlich (2008) stated that wind power is considered economically feasible only if subsidies, tax abatement, and environmental impact valuations are considered. Therefore, researchers believed that only renewable energy technology is cost-competitive with conventional energy sources (Painuly, 2001).

Raising the oil price, limited supplies of fossil fuel and energy sustainability issue have created a growing demand for renewable energy sources. Hence, in this study, the production of bioethanol (a type of biofuels – a renewable energy) by *Saccharomyces cerevisiae* (well known as Baker's yeast) was carried out using oil palm residues as substrates. The oil palm trunk (OPT) sap acted as a carbon source aided by palm oil mill effluent (POME) as nutrient supplier.

Bioethanol is a rapid and significant answer to the fossil fuel depletion crisis, significant reduction on greenhouse gases (GHG) emissions and global warming problems (Prasad et al., 2007; Hossain et al., 2008; Stanley et al., 2010; Triana et al., 2011; Amillastre et al., 2012; Dias et al., 2012). As reported by the United States Department of Energy (Rani et al., 2010), 1.3 units of energy are returned for every unit of energy required for bioethanol production (Stanley et al., 2010) and the main factor that needs to be considered when deciding to implement renewable energy is

adequate supply of feedstock (Painuly, 2001). Malaysia and Indonesia are the world's largest palm oil producers which contribute 90% to the world's palm oil export trade (Rupani et al., 2010), even though the oil palm is originally an African crop (Sulaiman et al., 2011). In Malaysia, oil palm occupies the largest area of planted land. As recorded by the Malaysian Palm Oil Board (MPOB, 2013), in the year 2012, 5.08 million hectares of areas has been planted with oil palm which was 1.5% higher as compared to the record of 2011. Most of these areas expansion occurred mainly in Sarawak at 5.3% increment (1.02 and 1.08 million hectares of area in 2011 and 2012, respectively). As a leader in palm oil producer in the world, Malaysia palm oil mills is processing 71.3 million tonnes of fresh fruit bunch (FFB) per year (Mekhilef et al., 2011).

The industry also produces large amount of residues from the oil extraction processes namely the mesocarp fibres, shells, empty fruit bunches (EFB) and POME (Yacob et al., 2006). According to Sulaiman et al. (2011), on a wet basis of FFB, 22% is actually EFB, 67% is discharged as POME, 13.5%, 6.0% and 5.5% are dumped as fibres, kernels and shells, respectively, and only about 22% is produced as the palm oil. In addition, a large quantity of cellulosic raw materials is generated in the form of felled trunks during replanting seasons. Disposal of these residues into land and waterways without pre-treatment would inevitably lead to pollution and other environmental problems.

1.2 Problem statement

Oil palm tree is replanted after 25 to 30 years. During replanting, a large quantity of OPT is generated. In spite of such large quantity of OPT produced, most

of them are left decayed or used as mulch. Meanwhile, a lot of liquid effluents are produced during the oil extraction processes. It is estimated that an average of 900 – 1500 litre of POME is generated for each tonne of crude palm oil (CPO) processed (Lam and Lee, 2011). POME has high biological oxygen demand (BOD), chemical oxygen demand (COD), suspended solids, oil and grease (Manickam et al., 2014). Therefore, it needs to be treated before being discharged into water streams. According to Lokesh et al. (2012) OPT sap contained 55.4 g/L sugar, and the amount of glucose rose up to 86.9% of the total free sugars, hence, it can be used as carbon source for the production of useful products (Chooklin et al., 2011; Lokesh et al., 2012). Meanwhile, POME contained high concentration of protein, carbohydrate, nitrogenous compounds, lipids and minerals (Rupani et al., 2010). Therefore, it can be used as the nutrient supplier for microorganism growth. However, the utilization of both residues (OPT sap and POME) as substrates (as carbon source and as nutrients supplier) in fermentation by microorganisms is less reported. During fermentation process, product yield depends on several process parameters conditions such as temperature, medium pH, agitation, speed, and nutrient availability. Although many studies have been conducted, there is still considerable divergence on the optimization particularly on these particular substrates.

POME and OPT sap are heterogeneous in nature and varies in characteristics, and as a consequence, the performance of any microorganism that grows in them might be affected. However, there has been no previous work describing the effect of kinetic model parameters fluctuation due to heterogeneity of substrates on the product yield during the fermentation process. Besides, the impact of each kinetic

model parameter on product yield particularly for a fermentation from oil palm residues (OPT sap and POME) is scarce in literature.

Currently, bioethanol fermentation at very high gravity (VHG – fermentation at very high glucose concentration) has gain increasing attention. It produces higher final concentration of bioethanol (Wang et al., 2013). If OPT sap is to be used as the substrate for a VHG fermentation, it needs to be concentrated at low temperature in order to avoid Maillard reaction or caramelization process. This can be achieved by lowering operating pressure in a rotary vacuum evaporator. However, evaporation model that considers both operating temperature and pressure simultaneously is not well established particularly for OPT sap concentrate. Nevertheless, VHG fermentation also has its drawbacks where yeast cells suffer higher osmotic stress at the early stage of fermentation (Kawa-Rygielska and Pietrzak, 2014), and higher ethanol toxicity at the later stage (Feng et al., 2012). It was reported that, in higher osmotic stress condition, yeast increased intracellular glycerol accumulation (Mager and Siderius, 2002) and produced more cytoplasmic trehalose (Bleoanca et al., 2013) during high ethanol toxicity. These mechanisms were achieved through several enzymatic processes. Therefore, activities of the enzymes during VHG fermentation need to be monitored.

1.3 Research objectives

The main objective of this study is to investigate the performance of bioethanol fermentation by *S. cerevisiae* using OPT sap supplemented with POME as substrates, and to study the yeast response mechanism on osmotic stress and ethanol

toxicity with regards to glycerol-3-phosphatase (G3Pase), and trehalose-6-phosphate phosphatase (TPP) enzymes activities.

The measurable objectives are:

- i. to optimize the process condition for bioethanol production by *S. cerevisiae* using OPT sap supplemented with POME as substrates using one-factor-at-a-time (OFAT) method and a statistical tool in shake flasks and in a stirred-tank bioreactor.
- ii. to predict the effect of fluctuation of kinetic model parameters on bioethanol yield due to heterogeneity of oil palm residues, and fluctuation of *S. cerevisiae* performance using Monte Carlo algorithm method.
- iii. to evaluate the impact of each kinetic model parameters on bioethanol yield using sensitivity analysis.
- iv. to develop an evaporation model of OPT sap concentrate behaviour in a rotary vacuum evaporator considering both temperature and pressure; and to study the response mechanism of *S. cerevisiae* at higher osmotic stress and ethanol toxicity during very high gravity (VHG) fermentation.

1.4 Scope of study

OPT sap is a potential feedstock for bioethanol production since it is rich in glucose, while POME is rich in nutrients required by Baker's yeast growth. Both OPT and POME are oil palm residues and they remain under-utilized. Therefore, in this study, bioethanol was produced by *S. cerevisiae* using OPT sap as carbon source, and POME as nutrient supplier in shake flasks and in a 2.5L stirred-tank bioreactor.

Many physical and chemical parameters influence bioethanol fermentation process. In this study, the effect of OPT sap to POME ratio, inoculum size, pH, and incubation time on bioethanol production by *S. cerevisiae* were investigated in shake flasks culture using OFAT method and response surface methodology (RSM) via face centered central composite design (FCCCD) in order to obtain the optimum condition. The effect of temperature, controlled pH, and agitation speed, on the bioethanol yield was studied in a 2.5L stirred tank bioreactor.

OPT sap and POME are heterogeneous in properties and might affect the performance of Baker's yeast as well as fermentation efficiency. Thus, the consistency of the result if the fermentation procedure is being reduplicated might be questionable. Therefore, the fermentation process should be evaluated using stochastic rather than deterministic approach. In this study, the effect of kinetic model parameters fluctuation on bioethanol yield was carried out using Monte Carlo algorithm. The variability of the parameters up to 3.0% relative standard deviation was carried out, and it is represented by normal distribution of 100,000 random numbers.

In addition, the impact of each kinetic model parameter on bioethanol yield was also evaluated by sensitivity analysis. Through this method, the kinetic model parameter that gave the most influence on bioethanol yield particularly for this study was determined.

In order to study the behaviour of OPT sap concentrate, evaporation of OPT sap at different temperatures and pressures was carried out using a vacuum rotary

evaporator. Several evaporation models considering simultaneous effect of temperature and pressure were developed and validated. The developed evaporation models were evaluated by determining the coefficient of determination (R^2), low root-mean-square error ($RMSE$), and variance during the VHG fermentation process. Enzymes activities particularly G3Pase, and TPP were determined during the VHG fermentation process in order to study the response mechanism of yeast to sustain its growth in high osmotic stress and high ethanol toxicity. Cell viability was also determined throughout the VHG fermentation studies.

1.5 Organization of the thesis

In order to make this study understandable, this thesis is divided into five chapters. An overview of energy sector and palm oil industry in Malaysia are discussed in **Chapter 1** (Introduction). The purpose of the chapter is to introduce the problems that the present study has solved. The problems statement (Section 1.2) provides some root and justification to identify the research directions to be conducted in this study. Chapter 1 also explains the objectives, and the scope of the study.

The successful of utilizing bioethanol as a fossil fuel substitute highly dependent on the economic feasibility of the process including the availability of feedstock and optimum process condition. Therefore, **Chapter 2** (Literature Review) reviews other researchers' studies on bioethanol fermentation process including the sources of feedstock, and environmental variables that affecting the bioethanol production (Section 2.1). Microorganisms that have the capability to produce bioethanol from glucose have also been reviewed in this chapter (Section 2.2). In

addition, the yeast response mechanism on osmotic stress and ethanol toxicity is also reviewed. The availability of oil palm residues particularly OPT sap and POME are reviewed and reported in this Chapter (Section 2.3). In order to study the VHG fermentation, OPT sap needs to be concentrated. Thus, a review on kinetic evaporation model has also been included. Due to heterogeneity of the oil palm residues, fermentation of OPT sap and POME needs to be analysed using stochastic rather than deterministic approach. Therefore, the usability of stochastic modelling using Monte Carlo simulation and sensitivity analysis are reviewed (Section 2.4). At the end of the chapter, the summary of literature review and the research gaps are described (Section 2.5).

Chapter 3 (Materials and Methods) describes how the study was carried out. All methods applied including list of equipment and chemicals are described in sufficient detail so that it can be reduplicated by others. The model and brand of the equipment and the grade of chemical are also reported. In order to make the methods used more understandable, the overall experiment flow diagram is also presented. The experimental procedures for bioethanol fermentation in both shake flasks culture and stirred-tank bioreactor, evaporation process of OPT sap, and the VHG fermentation are explained in detail. The statistical analysis techniques and analytical protocols are also described.

Chapter 4 (Result and Discussion) discusses in detail the experimental result and data analysis results. Discussions on the results are made and elaborated in details in this Chapter in order to demonstrate that all problems discussed in Chapter 1 have been solved in this study with the approaches and techniques explained in

Chapter 3. Chapter 4 is divided into four sections: (Section 4.1) Optimum conditions for bioethanol production by *S. cerevisiae* from oil palm residues (OPT sap and POME) in shake flasks culture and in a 2.5L stirred-tank bioreactor was determined; (Section 4.2) Stochastic modelling of the fermentation study is discussed in this Section. The effects of fluctuation of kinetics model parameters on bioethanol yield were investigated and elaborated; (Section 4.3) All kinetic model parameters do not give the equal impact on bioethanol yield. Therefore, impact of each kinetic model parameter is studied and detailed out in this Section; (Section 4.4) In this Section, results of VHG fermentation of oil palm residues by *S. cerevisiae* study are demonstrated. The activities of enzymes (G3Pase and TPP) are observed, reported and explained in detail. Prior to that, OPT sap was concentrated and the evaporation kinetic model of OPT sap concentrate considering temperature and pressure was developed and evaluated. The results are also demonstrated in this Section. All the results and discussions are supported with adequate supporting evidences and presented in form of graphical or table for better interpretation.

Chapter 5 (Conclusions) concludes the findings from the present study. Recommendations for future studies in the related field are also highlighted. To avoid confusion, contents of this chapter are arranged according to their appearance in Chapter 4.

CHAPTER 2

LITERATURE REVIEW

2.1 Bioethanol

Energy accessibility, supply and utilization play an important role in societies as well as industrial development. The need for energy increases endlessly mainly due to continuous increasing of population (Hossain et al., 2008). Besides, international relations, industrialization, economical, and political factors are also highly dependent on energy accessibility and cost. Over the past 50 years, the energy sector is extremely dependent on the utilization of fossil fuels (Bon and Ferrara, 2007). At this moment, about 80% of the world's energy demand is met by petroleum-based energy (Infantes et al., 2011). However, since early 1970s, the oil price had increased dramatically due to decision made by the Organization of the Petroleum Exporting Countries (OPEC) in order to control the production of oil (Galbe and Zacchi, 2002). Consequently, the world's interest in alternative fuels had increased significantly in order to reduce the dependency on fossil fuels.

Utilization of fossil fuels also lead to atmospheric pollution mainly caused by emission of greenhouse gases (GHG), especially carbon dioxide (CO₂) (Hossain et al., 2008). Kyoto protocol was established in 1997 with the intention to reduce pollution by limiting global net emission of CO₂. Over the past 150 years, a rapid increase in the volume of GHG emission has been observed. Consequently, this leads to alteration in the equilibrium of the earth's atmosphere. During this period, atmospheric CO₂ concentration had increased from 280 ppm to 365 ppm as reported

by Galbe and Zacchi (2002). Thus, alternative energy sources must be developed in order to reduce GHG emissions and global warming (Hossain et al., 2008; Amillastre et al., 2012). It was reported that the major sector that contribute to the CO₂ emission is transportation. Therefore, in order to reduce the volume of atmospheric CO₂ concentration, this sector should be given special attention. One of the approaches is by utilizing renewable energy (e.g.: biofuels/bioenergy) as the fossil fuel substitute. Generally, combustion of biofuels is cleaner and more environmentally friendly. Lower level of non-combusted hydrocarbons, carbon monoxide, nitrogen oxides and exhaust volatile organic compounds emission is resulted from combustion of biofuels (Galbe and Zacchi, 2002).

Therefore, in recent years, due to the environmental and economic reasons, biofuels have gained increase interest (Sveinsdottir et al., 2009). The demand for biofuels has drastically increased (Rani et al., 2010). However, An et al. (2011) found that the biofuel industry faces a few challenges: (i) The biomass tends to degrade during storage; (ii) major feedstock (e.g., dedicated energy crops and crop residues) can only be harvested in specific seasons but must satisfy year around demand; (iii) biomass characteristics and the price of fuel change over time. Furthermore, alternative technologies to convert biomass to biofuel, such as biochemical (e.g., enzymatic hydrolysis), thermochemical (e.g., steam explosion and pyrolysis), and bio-thermochemical (e.g., carboxylate pathway) processes are still under development.

Currently, the types of biofuels produced consist of; bioethanol, biomethanol, biobriquettes, biohydrogen gas and pyrolysis oil. In this study, we are focusing on

the bioethanol sector. Bioethanol is the main and most efficient biofuel and a raw material with wide range of applications in food, pharmaceutical, cosmetic, and petrochemical industry (Vučković and Pejin, 2007; Amillastre et al., 2012; Dias et al., 2012). Bioethanol is a rapid and significant answer to the fossil energy fuel depletion, global warming problems and significant reduction on GHG emissions (Prasad et al., 2007; Hossain et al., 2008; Stanley et al., 2010; Triana et al., 2011; Amillastre et al., 2012; Dias et al., 2012).

According to Oyeleke et al. (2012), bioethanol has a huge potential to replace gasoline in transportation. In fact, the idea of utilizing ethanol as fuel is not new. The oldest engine that utilized alcohol was reported in 1899 and about 4 million cars run with 25% bioethanol in gasoline between the world wars (Prasad et al., 2009). Brazil (pro-claimed as a front-runner in the use of renewable fuels) had started to substitute gasoline by bioethanol since 1975. Currently, around 24 million vehicles including cars, light commercials, trucks and buses fleet on Brazilian road run either by gasoline blend containing 22 – 24% bioethanol or 100% bioethanol (Bon and Ferrara, 2007).

Today, bioethanol is used mainly as an oxygenated fuel additive. At the moment, without any modification on the engine, all cars can be run by gasoline mixed with 10% of bioethanol and new cars can be run by up to 20% of bioethanol with a catalyst (Galbe and Zacchi, 2002). In addition, bioethanol capable to replace the diesel fuel to run compression-ignition engines. A mixture of diesel-bioethanol with emulsifier also can be used to reduce the emissions of exhaust (Galbe and Zacchi, 2002; Vučković and Pejin, 2007).

There are several other advantages of mixing bioethanol and gasoline. Bioethanol have higher octane number as compared to gasoline which is in the range of 96 – 113. Therefore, an increase in the percentage of bioethanol would increase the octane number of the fuel, subsequently reduce the need for toxic and octane-enhancing additives (Galbe and Zacchi, 2002). Bioethanol can also be used in the form of ethyl tertiary butyl ether as octane enhancer in order to substitute currently synthetically produced octane enhancers (Vuăuroviă and Pejin, 2007). A molecule of bioethanol contains carbon to oxygen ratio of 2:1. Thus, blending bioethanol and gasoline could oxygenate the mixture in order to achieve more complete combustion (Prasad et al., 2007; Oyeleke et al., 2012). Consequently, lower carbon monoxide and non-combusted hydrocarbons emission are produced. In the overall transport efficiency aspect, as reported by Galbe and Zacchi (2002) bioethanol was 15% more efficient in the optimized spark-ignition engines as compared to gasoline, and almost the same efficiency in compression-ignition engines as compared to diesel.

2.1.1 Bioethanol fermentation

About 90% of the world's ethanol production is produced from the fermentation of sugar (bioethanol), while only 10% is produced synthetically through hydration of ethene in vapour phase (Katada et al., 2008; Sveinsdottir et al., 2009). Bioethanol is produced through fermentation process of simple sugar by microorganisms (usually yeast or bacteria) (Prasad et al., 2007; Hossain et al., 2008; Prasad et al., 2009; Oyeleke et al., 2012). Table 2.1 summarizes some investigations that were carried out by other researchers on producing bioethanol through fermentation processes.

Table 2.1 A review on bioethanol production conditions and bioethanol yield from fermentation by several microorganisms and substrates

Substrates	Microorganisms	Conditions	Bioethanol Yield	Remarks	References
Sap wood of beech (<i>Fagus crenata</i>)	<i>Saccharomyces cerevisiae</i>	On orbital shaker at 100 rpm for 96 h at 35 or 40°C	14.8 g/l ethanol at 35°C 15.7 g/l ethanol at 40°C	Simultaneous saccharification and fermentation (SSF) process with Meicelase	(Itoh et al., 2003)
Coffee cut-stems	<i>Zymomonas mobilis</i>	incubated at 33°C for 30 h	240 L/t	Pre-treated with liquid hot water	(Triana et al., 2011)
Raw wheat flour	<i>Saccharomyces cerevisiae</i>	1.5 g/l dry yeast, pH 4.5, incubated at 35°C for 21 h	67 g/l ethanol	SSF process with amyloglucosidase	(Montesinos and Navarro, 2000)
5 Sweet potato peels	Combination of <i>Zymomonas mobilis</i> and <i>Saccharomyces cerevisiae</i>	shake and incubated at 28°C ±2°C for five days	6.5 g/ml ethanol Percentage yield of 12%	Separate hydrolysis and fermentation (SHF) process in shake flasks with <i>Gloeophyllum sepiarium</i> and <i>Pleurotus ostreatus</i>	(Oyeleke et al., 2012)
<i>Spirogyra</i>	<i>Zymomonas mobilis</i>	incubated for 96 hours at room temperature	9.70 % ethanol (v/v)	SHF process with α-amylase	(Sulfahri et al., 2011)

Table 2.1 (continued)

Substrates	Microorganisms	Conditions	Ethanol Yield	Remarks	References
Cassava peels	Combination of <i>Zymomonas mobilis</i> and <i>Saccharomyces cerevisiae</i>	shake and incubated at 28°C ±2°C for five days	11.97g/cm ³ ethanol. Percentage yield of 26%	SHF process in shake flasks with <i>Gloeophyllum sepiarium</i> and <i>Pleurotus ostreatus</i>	(Oyeleke et al., 2012)
Cashew apple juice	Immobilized <i>Saccharomyces cerevisiae</i>	Substrate concentration 10%, pH 6.0, temperature 32.5°C, inoculum level 8% (v/v) for 24 hours	7.62% ethanol yield	Batch process in shake flasks	(Neelakandan and Usharani, 2009)
Potato tubers (<i>Solanum tuberosum</i>) flour	<i>Saccharomyces cerevisiae</i>	incubated at 30°C for 48 h	56.8 g/l ethanol	Potato tubers were cooked and dried at 70°C prior to flouring. SHF process. Saccharification with glucoamylase	(Rani et al., 2010)
<i>Spirogyra</i>	<i>Saccharomyces cerevisiae</i>	incubated for 96 hours at room temperature	4.42 % ethanol (v/v)	SHF process with α-amylase	(Sulfahri et al., 2011)

Table 2.1 (continued)

Substrates	Microorganisms	Conditions	Ethanol Yield	Remarks	References
Agricultural raw materials	<i>Saccharomyces cerevisiae</i>	Incubated at room temperature in rotary shaker for seven days	Volume of ethanol produced from different raw materials in 250mL ethanol solution: Potato - 29 mL Sweet potato - 34 mL Cassava - 31 mL Fruit extract - 39 mL Boiled rice water - 24 mL Rice husk - 17 mL Rice straws - 12 mL Wood bark - 9 mL Sugar cane beets - 47 mL Waste Paper - 18 mL Saw dust - 11 mL Coconut pith - 5 mL Groundnut waste - 19 mL Leaf litter - 7 mL Maize husk - 19 mL	Batch process in shake flasks. Hydrolysis with amylase and cellulase produced by <i>Aspergillus niger</i> and <i>Trichoderma viride</i> prior to fermentation	(Prasad et al., 2009)
Commercial glucose solution	Immobilized <i>Saccharomyces cerevisiae</i>	incubated at 33.5°C for 28 h	Up to 72.5 g/L ethanol	Batch process in shake flasks.	(Călinescu et al., 2012)

Fermentation of sugar to produce bioethanol is a complex metabolic process. The simplified fermentation reaction equation of the bioethanol fermentation process is as shown in Equation (2.1) (Tadege et al., 1999):



Through this process, 1 mol of 6-carbon sugar (mainly glucose) is catabolized by microorganism into 2 mols of bioethanol. In addition, 2 mols of CO₂ are released. Bioethanol fermenting microorganism utilized glucose mainly through glycolysis pathway. The most common glycolysis process is through Embden–Meyerhof–Parnas (EMP) pathway (Bai et al., 2008; Lall et al., 2011; Sulfahri et al., 2011) as illustrated in Figure 2.1.

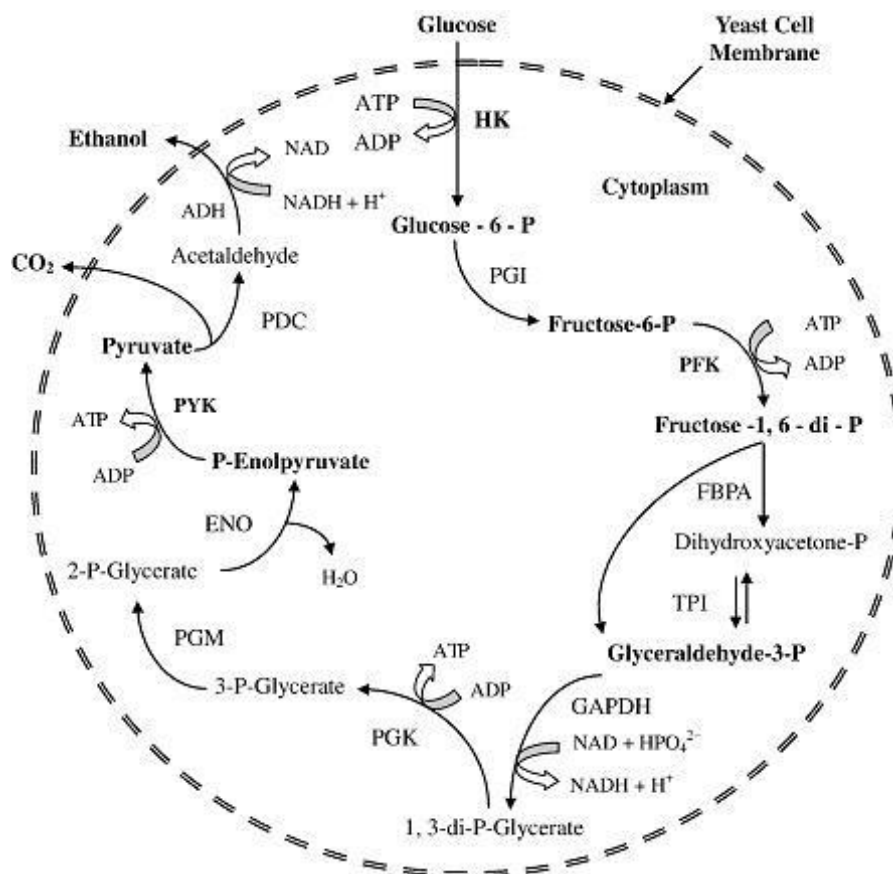


Figure 2.1 Metabolic pathway of bioethanol fermentation through EMP pathway (Bai et al., 2008). Abbreviations: HK: hexokinase, PGI: phosphoglucosomerase, PFK: phosphofructokinase, FBPA: fructose bisphosphate aldolase, TPI: triose phosphate isomerase, GAPDH: glyceraldehydes-3-phosphate dehydrogenase, PGK: phosphoglycerate kinase, PGM: phosphoglyceromutase, ENO: enolase, PYK: pyruvate kinase, PDC: pyruvate decarboxylase, ADH: alcohol dehydrogenase.

Basically, the metabolic pathway of bioethanol production from glucose can be divided into two parts: (i) conversion of glucose into pyruvate (glycolysis), and (ii) production of bioethanol from pyruvate. During the glycolysis process (Figure 2.2), the six-carbon atom of glucose is metabolized into two three-carbon molecules known as pyruvate via a series of enzymes. During this process, two molecules of adenosine triphosphate (ATP) are produced. In addition, two molecules of nicotinamide adenine dinucleotide (NAD^+) are converted into nicotinamide adenine dinucleotide hydrate (NADH).

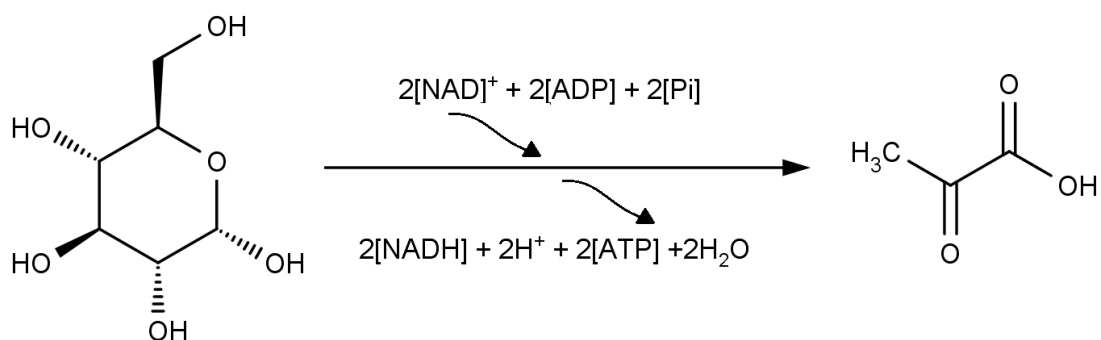


Figure 2.2 Conversion of glucose into pyruvate

Then, the molecule of pyruvate is converted into bioethanol with the release of CO_2 under anaerobic condition (Bai et al., 2008; Sulfahri et al., 2011) as shown in Figure 2.3. During this process, for each pyruvate molecule, an NADH is converted into NAD^+ with no change of ATP . Therefore, the overall conversion of glucose into bioethanol gives no net change of NADH and two molecules of ATP are produced. Theoretically, based on the stoichiometry of conversion, the reaction yields 0.511 g of bioethanol and 0.489 g of CO_2 for every gram of glucose consumed. In addition to bioethanol and CO_2 , various by-products are also produced mainly glycerol. In most cases glycerol was produced at a level of 1% (w/v) (Bai et al., 2008).

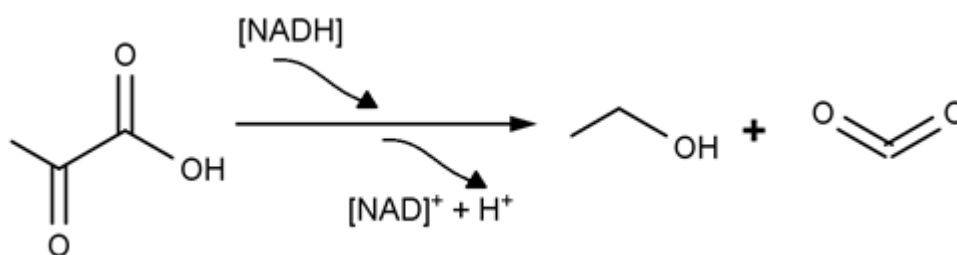


Figure 2.3 Conversion of pyruvate into bioethanol and carbon dioxide

2.1.2 Sources of feedstock

Basically, the feedstock for bioethanol production must contain sugar or starch and the sources varies (Galbe and Zacchi, 2002; Triana et al., 2011). They could come from municipal solid waste, agricultural residues, and other natural sources (Triana et al., 2011) including maize, cassava and cassava products, wheat crops, waste straw, guinea corn husk, rice husk, millet husk, sawdust and sorghum plants (Oyeleke et al., 2012).

The efficiency of utilization of bioethanol produced from biomass is highly dependent on economically feasible process. Thus, the net production cost must be equivalent to the corresponding cost for fossil fuels if not lower. The production cost of bioethanol is very much dependent on the cost of the feedstock, for instance, the use of sugar cane or maize as raw material, the feedstock cost was 40 – 70% of the total bioethanol production cost (Galbe and Zacchi, 2002). Accordingly, in order to lower the production cost, the use of cheaper raw materials is a must.

2.1.2 (a) Lignocellulosic materials

Lignocellulosic materials such as crop residues, grasses, sawdust, wood chips, solid animal wastes and industrial wastes are relatively cheaper sources of raw materials for bioethanol production (Prasad et al., 2007). Lignocellulosic material is the most abundant organic renewable component in biosphere and has a great prospect to be exploited for bioethanol production (Galbe and Zacchi, 2002; Kwon et al., 2011). About 50% of the biomass is lignocellulosic material with estimated production of $10 - 50 \times 10^{12}$ kg per year (Galbe and Zacchi, 2002) where plant cell walls are the prime source of lignocellulosic materials (Bon and Ferrara, 2007).

Lignocellulose consists of three main components: cellulose, hemicellulose and lignin. Cellulose and hemicellulose are composed of sugar molecules chains, which can be hydrolysed to produce monomer sugars for bioethanol production. Lignocellulosic materials are very high molecular weight and cross-linked aromatic macromolecule. Their structure is primarily represented by the physico-chemical interaction of cellulose (a linear glucose polymer) with hemicelluloses (a highly branched heteropolymer) and lignin.

Cellulose is the most abundant polysaccharide on earth. It is a highly ordered polymer of cellobiose (D-glucopyranosyl- β -1,4-D-glucopyranose). Cellulose polymer hydrolyses into its monomer; the glucose sugar. Hemicelluloses (also known as polysoses) are the linking material between cellulose and lignin. They are made of xylose, glucose, mannose, galactose and arabinose, as well as different sorts of uronic acids. Lignin is hydrophobic and highly resistant towards chemical and biological degradation. It acts as cement between the plant cells, and in the layers of the cell wall. Lignin and hemicelluloses form an amorphous matrix where the cellulose fibrils are embedded, thus protecting against biodegradation (Bon and Ferrara, 2007).

However, the existence of lignin makes the access of cellulolytic enzymes to cellulose difficult. Thus, it is necessary to decompose the network of lignin prior to the enzymatic hydrolysis (Itoh et al., 2003). Consequently, as compared to production from sugar-or-starch-containing crops, e.g. sugar cane or maize, production of bioethanol from celluloses and hemicelluloses are far more difficult making the cost to obtain sugars for bioethanol fermentation too high (Sun and